

Development of micro-pore optics for x-ray applications

Kotska Wallace[#], Marcos Bavdaz^{*}, Maximillien Collon[†], Marco Beijersbergen[†], Ray Fairbend[§],
Julien Seguy[§]

[#]Mechanical Engineering Department of ESA, ESTEC, Keplerlaan 1, PO Box 299, 2200 AG
Noordwijk ZH, The Netherlands

^{*}Science Payload and Advanced Concepts Office of ESA, ESTEC, Keplerlaan 1, PO Box 299, 2200
AG Noordwijk ZH, The Netherlands

[†] cosine Research BV, Niels Bohrweg 11, 2333 CA Leiden, The Netherlands

[§]Av. Roger Roncier, B.P. 250, 19106 Brive La Gaillarde Cedex, France

ABSTRACT

With Photonis and cosine Research BV, ESA has been developing and testing micro pore optics for x-ray imaging. Applications of the technology are foreseen to reduce mass and volume in, for example, a planetary x-ray imager, x-ray timing observatory or high-energy astrophysics. Photonis, a world leader in the design and development of micro pore optics, have developed a technique for manufacturing square channel pores formed from extruded glass fibres. Single square fibres, formed with soluble glass cores, are stacked into a former and redrawn to form multifibres of the required dimension. Radial sectors of an optic are then cut from a block formed by stacking multifibres and fusing them to form a monolithic glass structure. Sectors can be sliced, polished, etched and slumped to form the segment of an optic with specific radius. Two of these sectors will be mounted to form, for example, a Wolter I optic configuration. To improve reflectivity of the channel surfaces coating techniques have also been considered.

The results of x-ray tests performed by ESA and cosine Research, using the BESSY-II synchrotron facility four-crystal monochromator beamline of the Physikalisch-Technische Bundesanstalt (PTB), on multi-fibres, sectors and slumped sectors will be discussed in this paper. Test measurements determine the x-ray transmission and focussing characteristics as they relate to the overall transmission, x-ray reflectivity of the channel walls, radial alignment of the fibres, slumping radius and fibre position in a fused block. The multifibres and sectors have also been inspected under microscope and SEM to inspect the channel walls and determine the improvements made in fibre stacking.

Keywords: x-ray optic, Wolter, micro channel, micro pore

1. INTRODUCTION

1.1. Applications of the technology

Development of high resolution, lightweight, x-ray optics is required to reduce costs for future x-ray instruments proposed for ESA missions. Missions of interest are not only large, observatory type missions such as XEUS, but also planetary imagers such as the Mercury X-ray Spectrometer (MIXS). Both require reduction in the mass per collecting area available from x-ray from optics. The MIXS instrument is planned to fly on BepiColombo^{1,2}, one of ESA's cornerstone missions to be launched in 2011-2012 to investigate the origin and evolution of Mercury. X-rays are emitted from the Hermean surface due to x-ray fluorescence from the interaction of solar x-rays with the surface. Intensity and spectral distribution of the incident solar x-rays vary with the strength of solar output, increasing with solar flares. Using multi-spectral x-ray imaging should allow scientists to determine abundances of Na, Mg, Al, Si, Ca, K and Fe. This places a requirement on the instrument to cover the energy range 0.5-7.5 keV with an energy resolution less than 200 eV. In order to meet tight mass and volume constraints a robust, compact optic element for the instrument is required.

XEUS^{3,4} is being studied by ESA as a mission that to look at matter under extreme conditions, for instance in collapsed galaxy clusters and massive blackholes, investigating the nature of gravity, space and time. This astrophysics mission requires a very large aperture to form a permanent, space-borne, x-ray observatory 200 times more sensitive than XMM-Newton. X-ray optic elements will form a deployable aperture, from mirror modules known as petals, to form a very large effective area of approximately 30 m² at 1 keV, with angular resolution below 5''(goal 2''). X-ray optics are a critical technology to develop to allow a workable solution that will enable this mission to fly.

In the energy range of interest, 0.1 to 10 keV, only grazing incidence reflections can be exploited to focus an x-ray image. An ideal Wolter I optic uses two reflections, off a parabolic followed by a hyperbolic surface, to produce a real image (see Figure 2-2). To increase the effective imaging area the aperture is filled with concentric mirror shells, traditionally formed from glass or nickel plates, which are stacked in a nested structure with each shell individually mounted. By necessity the mirror shells are thin making them fragile, prone to distortion and difficult to align. The mount for each shell also constrains the inter-plate separation that can be achieved.

1.2. Technology development

As a consequence of the requirement to develop more robust x-ray optics, with a lower mass per collecting area, an activity supported by ESA has been developing compact, monolithic optics based on technology used to manufacture microchannel plates (MCP), which were principally used for night vision applications⁵. The technology addresses cost reduction via mass reduction; the volume of the optic is reduced and mounting is also made easier. Glass multifibres are formed from square microfibrils, which are then stacked into a radial configuration and fused, see Figure 1-1. Slices of this radial block can then be etched, to remove the core glass and form a regular pore pattern, and slumped to a predetermined shape. The pore top surfaces can now act as the reflecting surface with the radial arms providing strength and stiffness, preventing mirror distortions. Matched pairs, which have been slumped to different radii, can be used to form a Wolter I optic.

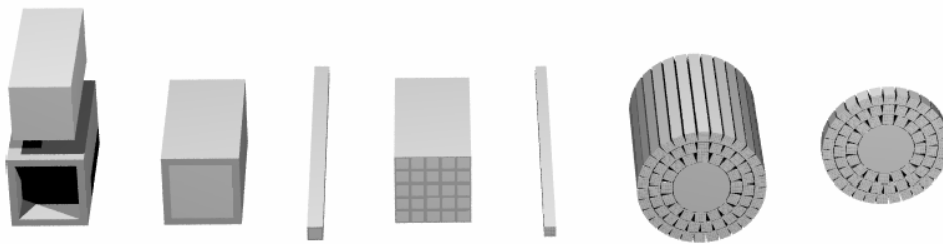


Figure 1-1; Manufacture of micro pore material used to form x-ray optic. Single fibres are drawn from a block of core plus cladding glass. These fibres are stacked and redrawn to form a multifibre. The secondary draw fibres are stacked into the required configuration and fused. The material can then be cut into slices to form x-ray optic elements.

In this paper we will briefly discuss the production of the x-ray optic samples before looking at the results of x-ray measurement campaigns recently carried out at the Physikalisch-Technische Bundesanstalt (PTB) lab at the Berliner Elektronenspeicherring-Gesellschaft für Synchrotronstrahlung (BESSY) synchrotron x-ray source.

2. MICRO PORE X-RAY OPTICS

The pore optics described give the ability to densely pack a very large number of very thin walled (10 µm) reflecting surfaces. The continuous surface of the monolithic, pore structure forms a rigid structure and the radial arms make the mirrors stiff enough to maintain the required shape (see Figure 2-1). Mounting problems are eased and an x-ray optic aperture can be built from segments mounted from blocks of x-ray optic.

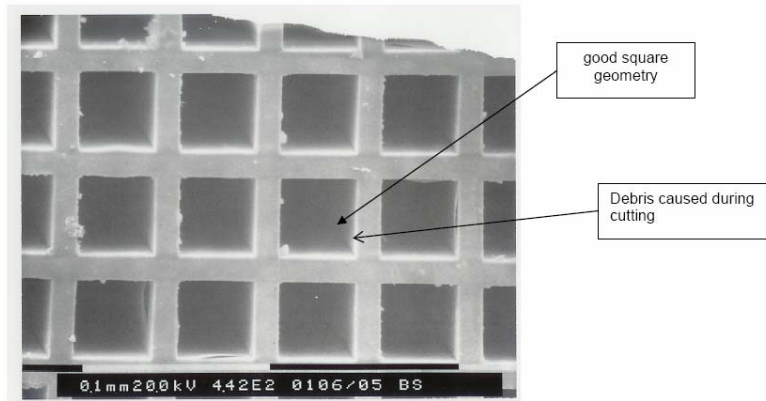


Figure 2-1: SEM image of etched, silicon, square pore material

When using conical surfaces to approximate the Wolter I optic the negative effect on imaging resolution can be made small if the reflecting surfaces are short, compared to the focal length. In addition, the azimuthal divergence of the mirror shells from spherical is acceptable as long as the width of each pore is smaller than the required focal spot size. Therefore, although a micro pore optic provides a concentric series of flat reflecting surfaces, it allows rays to be focused when the system is manufactured with small pores such that the reflecting surfaces' inclinations change with respect to radial distance from the aperture centre (see Figure 2-2).

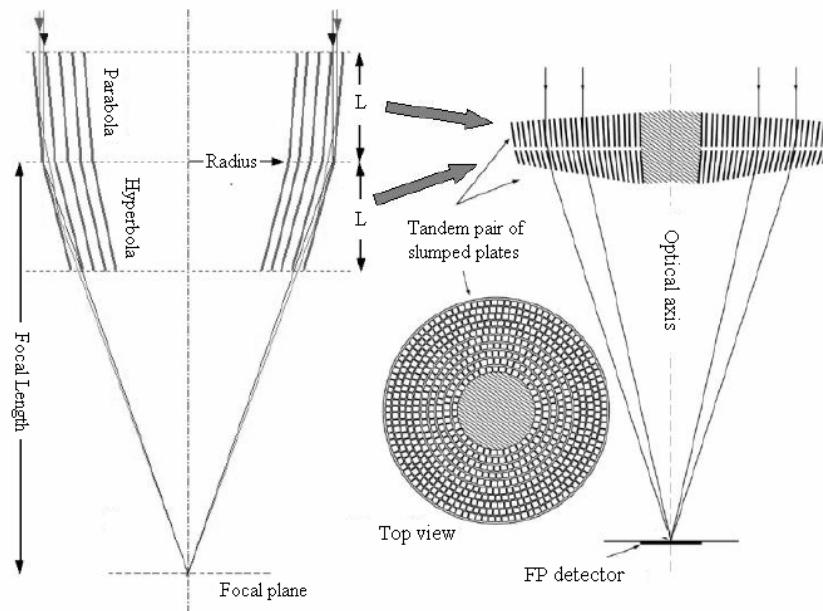


Figure 2-2: Square pore fibres are stacked radially and fused into a boule. Plates can be cut from this material and slumped under heat and pressure to form a conical approximation of the parabolic and hyperbolic sections of a Wolter I optic. The core material in the glass fibres is then etched away. The two sections can then be matched to form an optic with Wolter I approximation.

Improvements to the manufacturing process of square fibres^{6,7} have been made to improve the flatness and squareness of the surfaces and reduce surface roughness. The stacking procedure is also more closely monitored, with additional pre-selection of known (high quality) fibres, to form the best micro-pore material in a boule as possible. Slices are cut from this boule and polished, etched and slumped to form the required segments of the final aperture. The slice thickness required varies with distance from the aperture centre, however, slices of pore material for x-ray optic applications are in general thicker than those used for night vision applications. For the central regions of an optic, where the slice thickness needs to be greatest, this leads to difficulties in performing a clear etch through the full length of the fibres and also makes it more difficult to perform a uniform slump. Work has been conducted to refine the etch

process to allow deeper etching than previously performed, reducing blocked pores and remaining within surface roughness requirements, whilst maintaining a high level of heavy elements in the glass. Similarly, modifications are being made to the slumping process to provide a more uniform change of fibre angle against radial distance from the aperture centre.

In addition to improving the reflectivity of the pores, work has progressed in coating the optic to increase the x-ray reflectivity of the pore surfaces. The requirement is to coat with a uniform thickness between 20-200 nm and a surface roughness less than 2 nm rms, with a penetration depth up to length : diameter ratios of 1000. Nickel coated samples have been produced (Figure 3-5) using an electroless deposition method, which is currently being adjusted to improve the technique.

3. SAMPLE CHARACTERISATION

In order to measure improvements to the manufacturing process samples of square micropore material have been tested at the BESSY-II synchrotron facility four-crystal monochromator beamline of the PTB. A number of campaigns have been carried out during development of the manufacturing process and measurements have been made on samples of both multifibre material of various pore dimensions, on etched sectors and on slumped, etched sectors.

3.1. Multifibre samples

Measurements conducted on multifibres have looked at the quality of the draw, the accuracy of the stacking for the pore structure and the effect on reflectivity and transmission using different etch regimes. The sample is mounted within a vacuum chamber and irradiated by an x-ray beam at 3 keV. The beam size is adjusted such that it illuminates several pores of a microfibre. A series of measurements are then taken, at a number of points, of the reflection straight through the multifibre, with the fibre tilted by $\pm 0.1^\circ$ in tilt and then theta directions (i.e. reflecting of the top/bottom and then side walls). The transmission of the fibre is noted and indicates the percentage of blocked pores, due either to incomplete etching, etch by-products or debris that has trapped in the pores. From the quality of the reflected spot deductions are made concerning the geometry of the pore walls. For instance, double reflections (or more) are sometimes noticed in the radial direction or side by side. These can be due to, for instance, trapped bubbles/dirt in the draw, creating multiple focal lengths. The spot may also be elongated due to surface roughness or taper in the fibres. Figure 3-1 shows the reflected spots from 20 μm square pore multifibres of the same draw to demonstrate the manufacturing improvement performed in etching. The reflected spot on the left has been elongated and there are multiple peaks, which result in a HEW of 90 arcsec. The direct beam intensity during this measurement was 53,400, therefore the percentage at the spot maximum is only 1%. Using the improved etch, surface roughness and debris in the pores have been reduced; the HEW is decreased to 15 arcsec and there is a clean, single reflection peak with intensity 15% of the direct beam maximum.

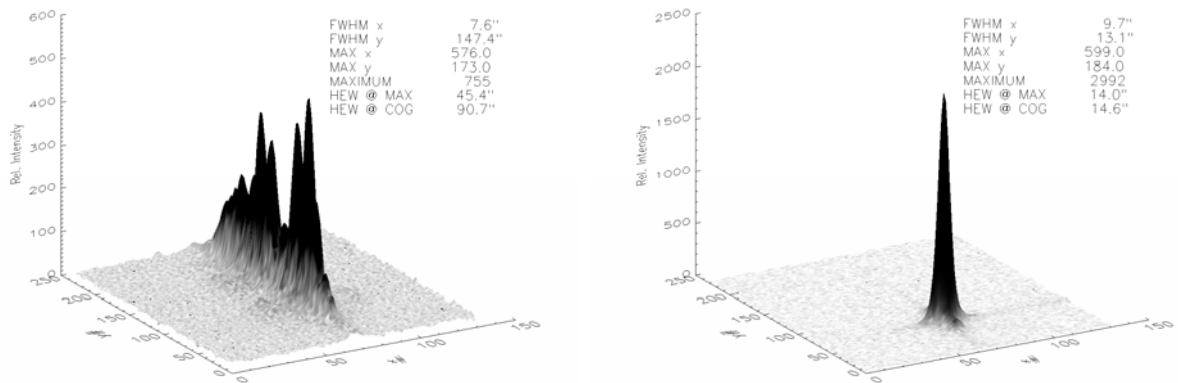
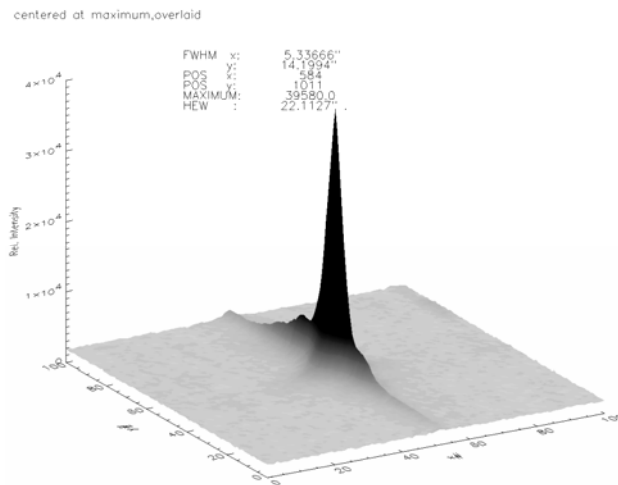


Figure 3-1: Recorded images of the reflection of 3 keV x-rays from a 100 x 100 μm square area in the centre of each multifibre. Both multifibres are from the same draw with 20 μm pores. The image on the left shows the reflection from a fibre etched early in the activity. The image on the right shows a reflection from the improved etch regime.

During measurements on multifibres a number of measurements are taken over the multifibre grid. The results of a scan can then be superimposed to look at the resultant spot size, overlaying either the raw images or the spots centred at their maximums (emulating a perfect optic). The results indicate the spot size that can be expected in the focused spot of a fully illuminated optic, due to the multifibre's manufactured characteristics, see the example in

Figure 3-2. Results indicate that fibre alignment can be regularly achieved within 2-7 arcsec and that when the spots are overlaid the resultant spot width ranges from 20-30 arcsec (HEW).



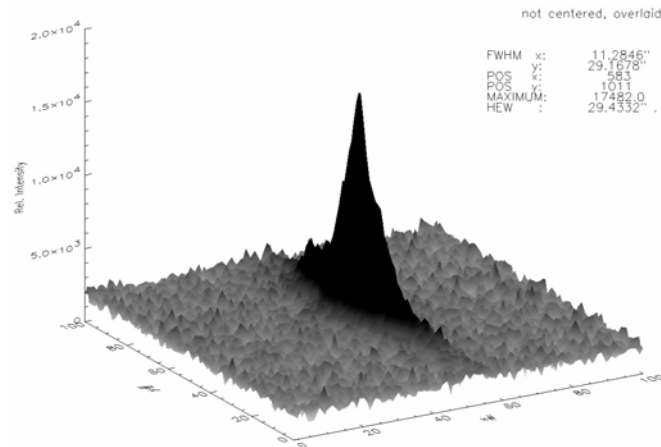


Figure 3-2: Overlaid spots reflected through a 46 μm square pore multifibre sample; 1 pixel = 1.77 arcsec. In the image on the left the spots have been centred on their maximums and on the right the raw images are overlaid.

The results of these campaigns have been to realise improved manufacturing practises for the multifibre material from which micro-pore optics will be formed. The process is also fine-tuned for each pore and fibre dimension ratio.

3.1.1. Nickel coated multifibres

The graph in Figure 3-3 shows the calculated reflectance from a perfect surface for silicon oxide and nickel. It can be seen that with 0.1° incidence there is little difference between the reflectivity of nickel and silicon oxide between 2 and 8 keV. However at 0.4° incidence (the incidence angle currently projected for the BepiColombo planetary imager) there is a small increase in the expected reflectivity for Ni over SiO at 3 keV and at 5 keV the reflectivity of SiO drops significantly, to around 10%, whilst the Ni reflectivity remains constant at more than 90% .

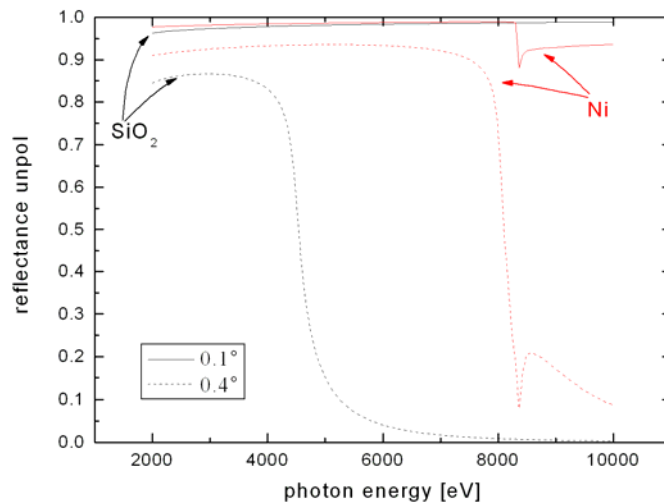


Figure 3-3: Reflectivity versus energy for 0.1° and 0.4° incidence angles for nickel and silicon oxide

Nickel coated multifibre samples have also been measured at the BESSY facility. Recently coated samples of 5 mm length, (Figure 3-5) were measured for reflection at incidence angles of 0.1° and 0.4° and energies of 3 keV and 5 keV. Transmission was comparable with uncoated samples of the same pore diameter, indicating that the pores had not been blocked by Ni deposits. The measured results at 3 keV showed that for 0.1° incidence the diameter of the overlaid reflected spots was approximately 23-24 arcsec (HEW), with little difference between diameters for centred or direct overlaying. At 0.4° incidence the spot width doubled to around 50 arcsec, with slightly less reflection for glass. At 5

keV and 0.4° incidence the reflected spot was still visible, indicating that sample has been successfully coated down the length of the pore, see Figure 3-4 . A test at 5 keV and 0.4° incidence did not result in a reflected spot.

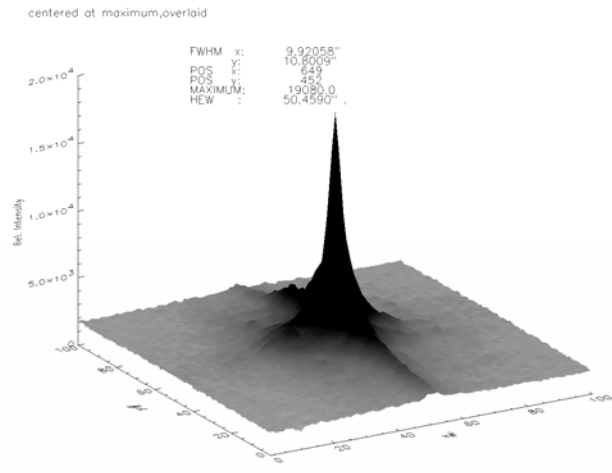


Figure 3-4: Reflection of 5 keV x-ray beam at 0.4° incidence, off 46 µm square pore, nickel coated multifibre

Confirmation of the x-ray results were obtained by cutting open one of the samples and making an analysis of the percentage ratios of Ni : P and Ni : Si at the surface, at 5 locations along the length of the fibre. Measured results for Ni : P were as expected, with 90% Ni to 10% P at each location. The measurement of Ni : Si gives an indication of coating uniformity and this showed that the current deposition method produces a coating that decreases in thickness along the length of the pore. Upon SEM inspection, evidence that the coat has lifted is visible at the entrance of some of the pores. Lifting may be due to the stresses induced by the cutting procedure or due to poor adhesion of the coating. A modification to the coating method is currently underway.

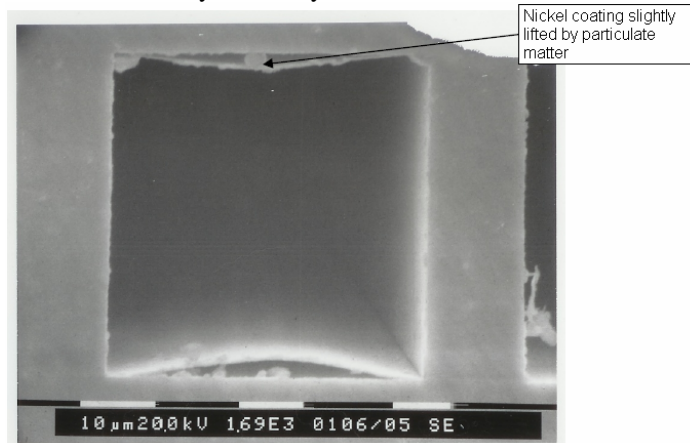


Figure 3-5: SEM image of a nickel coated, square pore multifibre showing some evidence of coat lifting at the pore entrance, possibly due to cutting procedure or bad adhesion inherent to coating process.

3.2. Sector samples

X-ray measurements have been performed on both slumped and unslumped sectors. The objective of the measurements is to look at the alignment of the multifibres within the sector and to determine if the slumping operation deteriorates the multifibre alignment or reflectivity of the pore walls. The uniformity of the slump is also measured.

3.2.1. Unslumped sectors

The unslumped, radial sector is mounted within a vacuum chamber and irradiated with a 3 keV x-ray beam of approximately $100 \times 100 \mu\text{m}$. A matrix of measurements is taken sampling across the surface of the sector. At each measurement position the sector is aligned for maximum transmission through the local pore structure and the corresponding tilt and theta angles (see Figure 3-6) are recorded. The sample is then tilted 0.1° in the theta direction and if a sidewall reflection is generated then the sample is rotated around tilt until this is gone, to give maximum reflection from one pore wall only. The measured reflected spots give the maximum reflection off the pore wall used for focusing x-rays in the final optic. The measurements of the unslumped plate are compiled and the centre and optical axis are calculated.

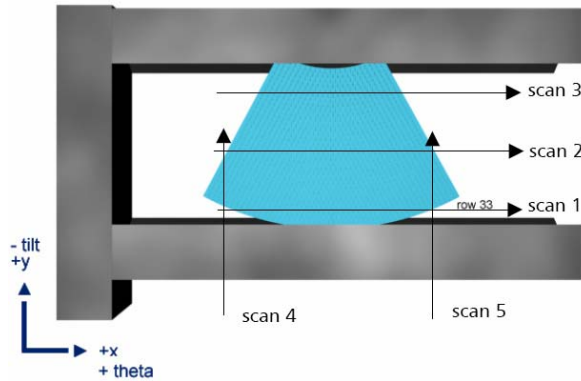


Figure 3-6: Mounting and coordinate system for measurements on sector samples. The x-ray beam is incident from the z-direction.

Several unslumped sectors have been measured and improvements noted in the quality of alignment of the multifibres within the sector. Recent measurements of a 5mm thick sector, containing square multifibres of $20 \mu\text{m}$ pores, stacked in a mould of inner radius 20 mm and outer radius 50 mm, show that individual multifibres are co-aligned over a whole sector to 1 arcmin, with a standard deviation of 0.7 arcmin. The reflections have about 25% of the intensity of the direct beam. Figure 3-7 demonstrates the recently measured reflections from a sector and Figure 3-8 is a map showing the measured angles of multifibres within a sector.

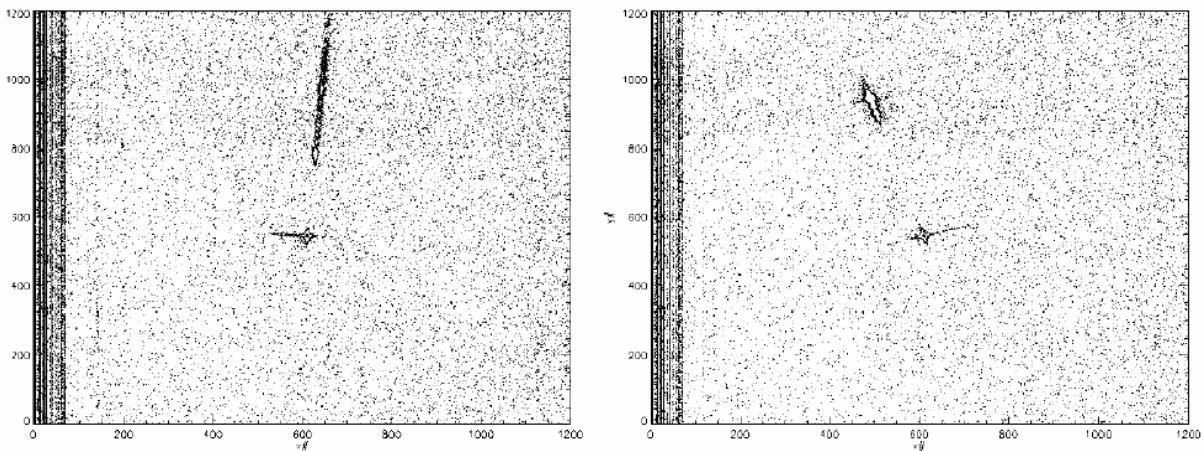


Figure 3-7: Two typical reflections measured at 0.1° incidence angle on a 5 mm thick sector containing $20 \mu\text{m}$ pores; one pixel corresponds to 1.76 arcseconds. The centre spot is the direct beam. The intensity scale is logarithmic.

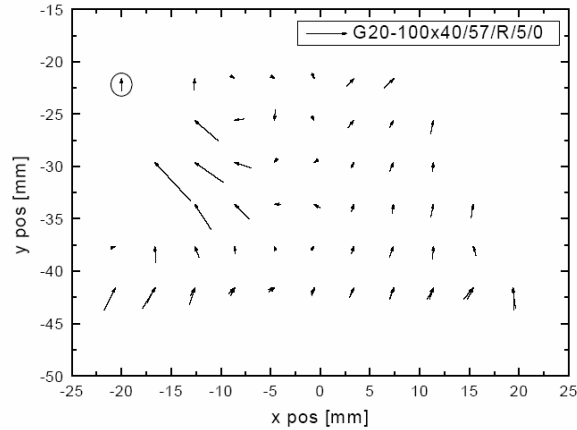


Figure 3-8: Projection of the measured angles, where the arrows indicate the direction in which the fibre is tilted at the measurement location. Arrow length represents the angle over which the fibre is tilted in that direction. The encircled arrow is artificial and represents a tilt angle of 1 arcmin. Multifibre alignment errors can be seen on the left side of the sector.

An improved metrology system is currently being installed in the manufacturing stacking system to reduce multifibre misalignment when stacking radial sectors. However these results show that the alignment of the fibres in an unslumped sector is currently sufficient for an x-ray optic with 1-2 arcmin resolution.

3.2.2. Slumped sectors

Measurements have been performed on sectors slumped, without modification to the current manufacturing process, for to 2 different radii: 4 m and 1.3 m. The slumped sectors are cut from the same boule as the unslumped sector discussed in 3.2.1 and therefore have the same thickness, pore size and inner/outer radii. The x-ray measurements are also sampled in the same manner across the surface of each sector. The results of these measurements are abbreviated in Figure 3-9 and Figure 3-10 for a 4 m and a 1.33 m slump respectively. These results show that, before the modifications currently being implemented by the manufacturer, the slumping process is not uniform across the sector and some misalignment of the multifibres is induced. The problem has arisen due to the greater thickness of the plates used when compared to standard micro-channel plates and occurs mainly at the outer radii of the sector. When the outer radii measurements are discarded from datasets, spot sizes below 4 arcmin result at distances within 3% of the design focal distance.

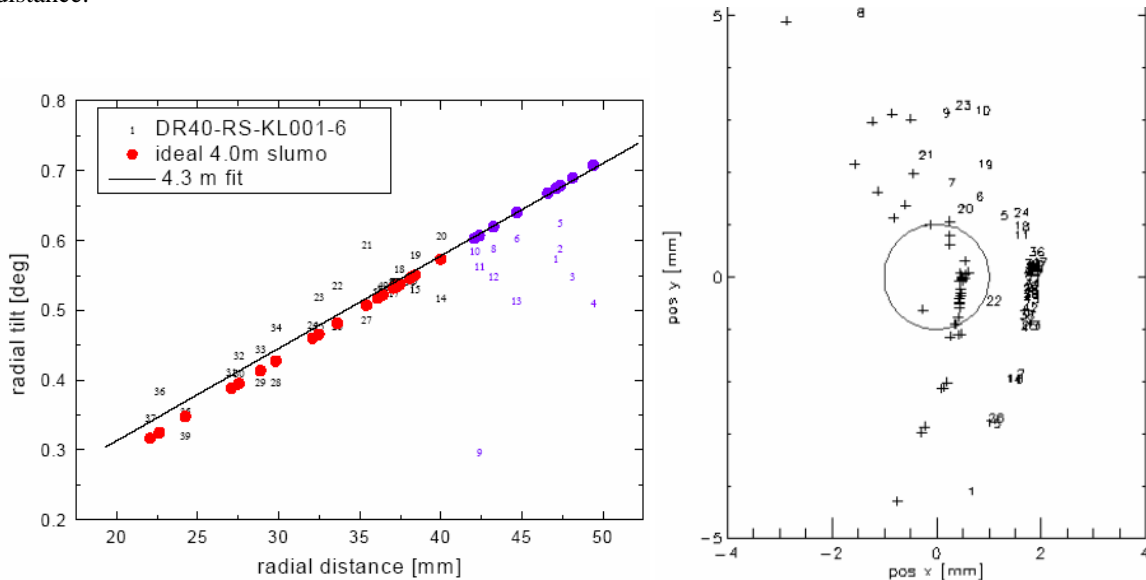


Figure 3-9: The graph on the left plots measured angles as a function of radial distance. Black numbers represent measured points and red marks indicate the design radius of 4 m. Blue values indicate fibres beyond a sector radius of 40 mm and have been omitted from the fit, which yields a slump radius of 4.3 m. Results of a ray trace with the azimuthal tilt artificially set to zero. The position of the intersection plane is defined by the smallest spot diameter along the beam formed by the best 50% of fibres. The HEW circle has a diameter of 1.68 arc min at a focal distance of 4120 mm.

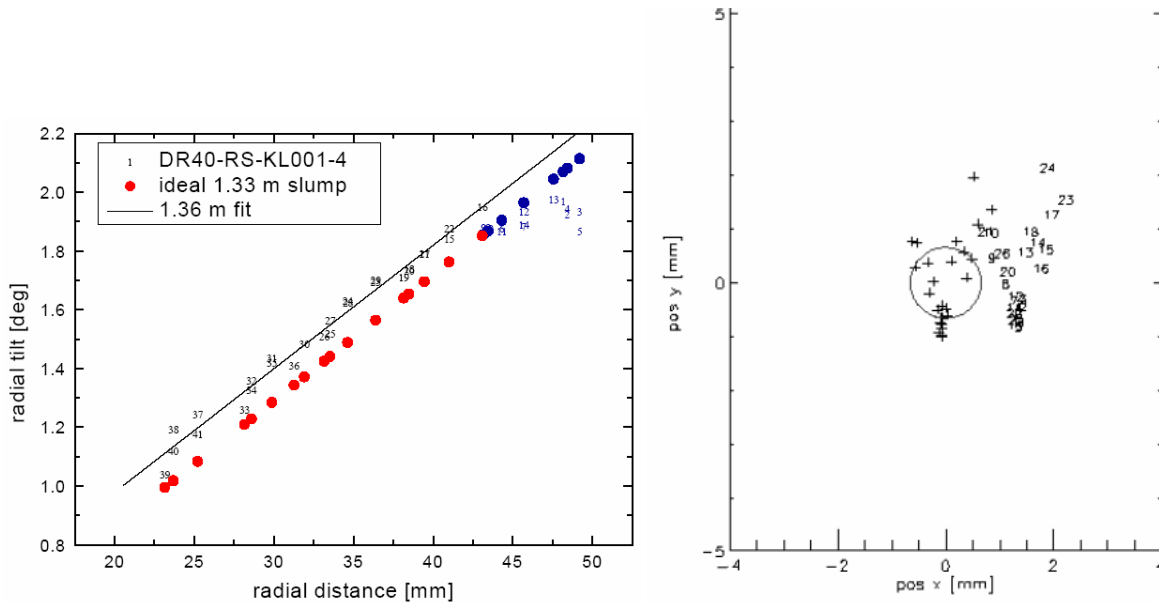


Figure 3-10: The graph on the left plots measured angles as a function of radial distance. Black numbers represent measured points and red marks indicate the design radius of 1.3 m. Blue values indicate fibres beyond a sector radius of 43 mm and have been omitted from the fit, which yields a slump radius of 1.36 m. Results of a ray trace with the azimuthal tilt artificially set to zero. The position of the intersection plane is defined by the smallest spot diameter along the beam formed by the best 50% of fibres. The HEW circle has a diameter of 3.56 arc min at a focal distance of 1270 mm

4. CONCLUSIONS

The measurement campaigns conducted thus far on square pore multifibres, and on slumped and unslumped sectors produced from radial stacking of multifibres, have demonstrated some of the improvements in current manufacturing process. The results are encouraging and indicate that the design requirements for a planetary imager x-ray optic can be reached. Modifications to the manufacturing processes for stacking and fusing square single fibres, plus installation of new metrology and fibre selection processes on the draw tower, have resulted in higher quality multifibres. The etch process has been adapted for the longer fibre length required for x-ray optics and a method has been found for coating the longer fibres with nickel to increase reflectivity.

Manufacturing process improvements have been highlighted and are currently under installation. These include:

- improvements to the stacking system for radial stacking of square pore multifibres into sectors;
- modifications to the slumping tool and oven to perform uniform slump over thick sectors;
- fine tuning of the etch process to be performed for each pore diameter.

ACKNOWLEDGEMENTS

We would like to express our thanks to the Physikalisch Technische Bundesanstalt for the testing provided at BESSY, Thanks also to the XEUS Science Advisory Group for the continued interest in the development of new generation x-ray optics for astrophysics missions.

REFERENCES

1. Revised and updated by the Payload Review Committee, “*Bepi-Colombo Science Requirements for the Payload of the Mercury Planetary Orbiter*”, SCI-PB-RS-1156, Version 2.2, ESA, Feb. 2004
2. C. Erd et al, “*BepiColombo Payload Study Document*”, SCI-A/2002/007/Dc/CE, CR_BC_TN15, iss. 4, rev. 1, ESA, February 2004
3. Marcos Bavdaz et al, “Progress at ESA on High Energy Optics technologies”, *Optics for EUV, X-Ray, and Gamma-Ray Astronomy*, O. Citterio, Stephen L. O'Dell, Editors, Proc. SPIE, Vol. 5168, pp. 136-147 Jan. 2004
4. Stefan Kraft et al, “Development of x-ray pore optics: novel high-resolution silicon millipore optics for XEUS and ultralow mass glass micropore optics for imaging and timing”, *Design and Microfabrication of Novel X-Ray Optics II*, Anatoly A. Snigirev, Derrick C. Mancini, Editors, Proc. SPIE Vol. 5539, pp. 104-115, Nov. 2004
5. “*Development of microchannel plates for UV and x-ray imaging systems*”, Photonis Summary Report, ESTEC Contract # 12193/96/NL/SB, June 2000
6. Marcos Bavdaz et al, “X-ray optics – new technologies at ESA”, *X-ray and gamma ray telescopes and instruments for astronomy*, Joachim E. Truemper, Harvey D. Tananbaum, Editors, Proc. SPIE Vol. 4351, pp. 421-432, March 2003
7. M. Collon et al, “*Metrology for square glass fibres for micropore x-ray optics*”, EOS Conference on Industrial Imaging and Machine Vision, Munich, June 2005